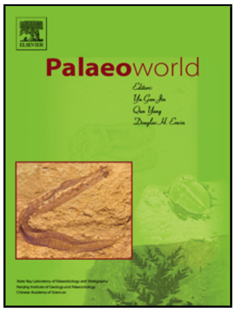

Title: Additional cricetid and dipodid rodent material from the Erden Obo section, Erlian Basin (Nei Mongol, China) and its biochronological implications

Author: Qian Li

PII: S1871-174X(18)30076-3
DOI: https://doi.org/10.1016/j.palwor.2018.09.003
Reference: PALWOR 468

To appear in: *Palaeoworld*

Received date: 22-5-2018
Revised date: 11-7-2018
Accepted date: 6-9-2018

Please cite this article as: Li, Qian, Additional cricetid and dipodid rodent material from the Erden Obo section, Erlian Basin (Nei Mongol, China) and its biochronological implications.Palaeoworld https://doi.org/10.1016/j.palwor.2018.09.003

Additional cricetid and dipodid rodent material from the Erden Obo section, Erlian Basin (Nei Mongol, China) and its biochronological implications

Qian Li [a, b]

[a] Key Laboratory of Vertebrate Evolution and Human Origins of Chinese Academy of Sciences, Institute of Vertebrate Paleontology and Paleoanthropology, Chinese Academy of Sciences, Beijing 100044, China

[b] CAS Center for Excellence in Life and Paleoenviroment, Beijing 100044, China

E-mail address: liqian@ivpp.ac.cn

Abstract

New cricetid (*Cricetops dormitor*, *Eocricetodon* sp., *Eucricetodon* cf. *E. wangae*, *Pappocricetodon schaubi*) and dipodid (*Allosminthus gobiensis* n. sp., *Allosminthus ernos*, *Allosminthus uniconjugatus*, *Allosminthus* cf. *A. majusculus*, *Primisminthus shanghenus*, *Sinosminthus* sp.) occurrences from the “Lower Red”, “Middle Red”, “Middle White” and “Upper White” beds of the Erden Obo section in Nei Mongol, China are reported. They are first discovered in these horizons. On the basis of the comparison of the rodent assemblages, we consider that the age of the “Upper White” beds is early Oligocene, the age of the “Middle Red” and “Middle White” beds is probable more similar to the age of late Eocene Houldjin Formation and lower part of Chaijiachong Formation, and the age of the “Lower Red” beds is correlative to the Sharamurunian. The diversity of ctenodactyloid, dipodid, and cricetid appears to change, and the turnover in rodent fauna possibly responded to the environmental and climate change towards the end of middle Eocene.

Keywords: Mammalia; Rodentia; Eocene; Oligocene; Nei Mongol; Erden Obo

1. Introduction

The Erden Obo section is a key to the understanding of the stratigraphy and faunal evolution from Paleocene to early Oligocene in the Erlian Basin. The Central Asiatic Expeditions from the American Museum of Natural History (Granger, 1928; Radinsky, 1964), the Sino-Soviet Paleontological Expedition (Chow and Rozhdestvensky, 1960), the Regional Geological Survey of Nei Mongol Autonomous Region, and the Institute of Vertebrate Paleontology and Paleoanthropology (IVPP) investigated the Erden Obo section during the last century. However, different researchers divided the strata of the Erden Obo into different stratigraphic formations and ages (Osborn, 1929; Chang, 1931; Pei et al., 1963; Jiang, 1983; Qi, 1990; Qiu and Wang, 2007). As a result, the lithostratigraphic and biostratigraphic units of the Erden Obo section is poorly constrained in terms of both superpositional relationships and dating independent of fossils. Correlation of these units remains controversial, which hampers the understanding of faunal evolution and biotic responses to environmental changes, both regionally and globally.

From 2007 to 2012, a comprehensive investigation in Erden Obo section that included lithostratigraphy, biostratigraphy, and paleomagnetic study were carried by a joint team from IVPP, American Museum of Natural History, Carnegie Museum of Natural History, and Northern Illinois University. About five hundreds of teeth, numerous maxilla and jaw fragments of rodent from the Erden Obo section have been collected from several field seasons. Only a few rodent specimens were reported from the Erden Obo section in previous studies (Wang, 2001, 2007b). Recently, we systematically reported ctenodactyloid rodents from the Erden Obo section (Li, in press), dipodid and cricetid materials from the “Upper Red” beds of the Erden Obo (Li, Q. et al., 2016a, 2017), and the rodent assemblages from the lower part of the Erden Obo section (Li et al., 2018). In this study I will document exclusively the new materials of dipodid and cricetid rodents of the Erden Obo section (Fig. 1). The new data reported here add new information on the temporal and geographic distribution of the cricetids and dipodids, and also provide important evidence for stratigraphic division and age estimation of the fossiliferous beds. The diverse species from the different horizons will undoubtedly help to understand the radiation and evolution of this Paleogene rodent group of Asia.

2. Material and methods

All newly described specimens were collected in several field expeditions during 2007–2012, and they were collected by surface prospecting and screen-washing of about eight tons of sediment from several beds in the Erden Obo where stratigraphic data were systematically record. Dental terminology in the description illustrated in Fig. 2 generally follows Li, Q. et al. (2017) for dipodids and Li et al. (2016a) for cricetids. Measurements of teeth were taken using a reticle with an accuracy of 0.1 mm mounted in an Olympus SZX7 microscope. SEM photographs were taken using a JSM-6100 SEM machine at the Key Laboratory of Vertebrate Evolution and Human Origins, Institute of Vertebrate Paleontology and Paleoanthropology, Chinese Academy of Sciences. All fossil specimens collected are housed in IVPP, and are available for examination by qualified researchers.

3. Geological settings

Osborn (1929) first reported the Erden Obo section based on Granger's and Spock's field notes. He subdivided the deposits in the section into 8 units, termed in descending order as the "Upper White", the "Upper Red", the "Middle White or Gray", the "Middle Red", the "Lower White" , the "Lower Red", the "Basal White", and the "Basal Red". The lithological division and correlation of the beds in Osborn (1929) have long been a matter of uncertainty (Chang, 1931; Pei et al., 1963; Jiang, 1983; Qi, 1990; Qiu and Wang, 2007). Because of the complicated research history and potential sedimentary hiatuses in the sequence, the formal division and correlation, including naming of the stratigraphic units, have not yet to be completed (Wang et al., 2012). For the present, we continue to use the descriptive term of Osborn to denote the beds where the fossils reported here came from. However, it should be noted that the lithological assignment and age estimate are probably different from those suggested by Osborn.

4. Systematic paleontology

Rodentia Bowdich

Family Dipodidae Fischer de Waldheim

Primisminthus shanghenus Tong, 1997

(Fig. 3A)

Specimen: Left M1 (IVPP V 25036).

Locality and horizon: Erden Obo, Nomogen, Siziwangqi, Nei Mongol, China; "Lower Red" beds.

Description and comparison: The tooth measurement (length/width in mm) is 1/0.95. The low-crowned M1 has three roots. M1 is trapezoidal in outline, and is slightly wider posteriorly than anteriorly. The contact facet on the anterior surface is consistent with presence of a small P4. A short anterior arm of the protocone exists between the paracone and the protocone. The protoloph II is absent, and the parastyle of M1 is weak. The metaloph is short, and tends to the hypocone but does not connect to the hypocone. The most remarkable character is that the protoloph II is weak and the anterior arm of the hypocone is extending to the center of the tooth. A small mesostyle and mesocone are present.

The new specimen from the Erden Obo has a complete anterior arm of the protocone on M1 that forms the only connection between the paracone and the protocone, no protoloph II on M1, a lophate metacone extending to hypocone, a weak posterior arm of the protocone, and a long anterior arm of the hypocone. All the features are identical with those of *Primisminthus shanghenus*. The size of the new specimen falls into the range of variation of *P. shanghenus* (Tong, 1997).

Allosminthus Wang, 1985

Allosminthus uniconjugatus (Tong, 1997)

(Fig. 3B)

1997 *Banyuesminthus uniconjugatus* – Tong, p. 137, text-fig. 64, pl. 11, figs. 18-23.

2008a *Allosminthus uniconjugatus* – Wang, p. 21.

Specimen: Left M1 (IVPP V 25037).

Locality and horizon: Erden Obo, Nomogen, Siziwangqi, Nei Mongol, China; "Lower Red" beds.

Description and comparison: This tooth measures (length/width in mm) 1.04/1.03. Four main cusps in M1 are distinct and crests are low. The anterior cingulum is present in M1. The anterior arm of the protocone is complete and extends labially to connect the anterior part to the paracone. The protoloph II is lack. The metaloph is complete and connected to the anterior arm of the hypocone. The posterior arm of the protocone is weak.

Compared to the holotype of *Allosminthus uniconjugatus* (Tong, 1997; Wang, 2008a; Daxner-Höck et al., 2014) from the Rencun Member of the Hedi Formation of Henan Province, the protoloph II of the specimen reported here is weaker and the occlusal surface of M1 is more nearly square. The new specimen differs from *Primisminthus shanghenus* that is from same horizon in being well developed precingulum that joins a small parastyle at the anteriolabial corner of the tooth, and in having longer metaloph that extends to the anterior part of the hypocone and shorter anterior arm of the hypocone.

Allosminthus gobiensis n. sp.
(Fig. 4)

2008a *Allosminthus* cf. *A. diconjugatus* – Wang, p. 22, fig. 1.
2017 *Allosminthus* cf. *A. diconjugatus* – Li, Q. et al., p. 8, fig. 7.

Etymology: The specific name is derived from Nei Mongol Gobi, the type locality of the species.

Type specimens: Holotype: right maxilla with broken P4-M1 (IVPP V 25038.1); paratype: right mandible with m1-3 (IVPP V 25038.2).

Type locality and horizon: Erden Obo, Nomogen, Siziwangqi, Nei Mongol, China; “Middle Red” beds.

Referred specimens: Left mandible with m2 (IVPP V 25038.3), right mandible with m2-3 (IVPP V 25038.4), left m1 (IVPP V 25038.5), left m2 (IVPP V 25038.6-9), and right m2 (IVPP V 25038.10) from the type locality and horizon. Left M1 (IVPP V 25039.1), right M1 (IVPP V 25039.2-5), left M2 (IVPP V 25039.6-7), right M2 (IVPP V 25039.8-9), left m1 (IVPP V 25039.10-12), right m1 (IVPP V 25039.13), left m2 (IVPP V 25039.14-16), right m2 (IVPP V 25039.17-18), and left m3 (IVPP V 25039.19-21) from Erden Obo, Nomogen, Siziwangqi, Nei Mongol, China; “Middle White” beds.

Differential diagnosis: *Allosminthus gobiensis* differs from *A. uniconjugatus* and *A. majusculus* in having a complete protoloph II in M1-2. It differs from *A. ernos* and *A. khandae* in having a distinct protoloph II in M2. It differs from *A. minutus* in having larger size, a shorter mesoloph in M1-2 and a more distinct mesoconid. It differs from *A. diconjugatus* in having a complete protoloph II on M1-2 that enclosed a deep fossette between the protocone and paracone, a weaker mesocone and a longer mesoloph, and more developed metalophid on m2 that is connected to the anterolophid.

Description: One right mandible with m1-3 is preserved (Fig. 4B). The anterior edge of the masseteric fossa of IVPP V 25038.2 extends to between m1 and m2, and a distinct mental foramen is anteroventral to m1 on the mandible (Fig. 4C).

A small P4 is present in IVPP V 25038.1 (Fig. 4A). It is single-rooted.

The M1 is trapezoidal in outline. The complete anterior arm of the protocone joins the anterior part of the paracone, and the protoloph II connects with the posterior arm of the protocone (Fig. 4D). They enclose a deep fossette between the protocone and paracone. The metaloph joins the hypocone (present in 4 specimens of a total of 6 specimens) or the anterior arm of the hypocone (2/6). The mesoloph is usually long and reaches the labial border. A small mesostyle is present in some specimens. The entoloph is continuous.

The M2 is also trapezoidal in occlusal outline, longer than wide and narrower posteriorly than anteriorly. The M2 is similar to M1, and the anterior arm of the protocone and the protoloph II are also complete (Fig. 4E, F). The anteroloph is more developed than that in M1. The mesoloph is medium and shorter than that in M1.

The m1 tapers anteriorly, and an isolated anteroconid is present. The complete posterior arm of the protoconid is U-shaped and connected with the protoconid. The ectolophid is low and a distinct mesoconid is present on the ectolophid (Fig. 4B, G). The mesolophid is weak. The hypolophid is complete and extends to the anterior arm of the hypoconid. The posterolophid is well-developed and reaches the base of the entoconid. A small mesostylid is present in IVPP V 25038.5 (Fig. 4H).

The lingual anterolophid of m2 is longer than the labial one. The anterior arm of the protoconid and the metalophid are connected to the anterolophid, and the posterior arm of the protoconid extends to the base of the metaconid and closes the trigonid (11/13). The mesolophid is medium of length (6/13) (Fig. 4I) or weak (7/13) (Fig. 4J). The mesoconid is weaker than that in m1. The shape of the talonid is similar to that of m1.

The m3 is the smallest lower molars. The metalophid is complete and connects with the anterior arm of the protoconid, but the posterior arm of the protoconid varies from long (2/5) to short (3/5). There are no closed trigonid and mesolophid. The hypolophid is complete (Fig. 4K).

Comparisons: The new materials from the “Middle Red” and “Middle White” beds share the following features with *Allosminthus*: crown brachyodont, with obtuse main cusps and low crests, a strong anterior arm of the protocone of M1 connected with the paracone, a metaloph of M1-2 extended to the anterior arm of the hypocone or the hypocone, and a complete hypolophid in lower molars.

Allosminthus includes six previously described species: *A. ernos* (Wang, 1985), *A. majusculus* (Wang, 1985, 2008a), *A. diconjugatus*, *A. uniconjugatus* (Tong, 1997; Wang, 2008a; Daxner-Höck et al., 2014), *A. minutus* and *A. khandae* (Daxner-Höck, 2001; Wang, 2009; Daxner-Höck et al., 2014). *A. gobiensis* can be clearly distinguished from *A. uniconjugatus* and *A. majusculus* in having a complete protoloph II in M1-2. The protoloph II is pronounced in M1 of *A. ernos* and *A. khandae*, but the protoloph II in M2 of *A. ernos* is never present and it is occasionally with a weak protoloph II in *A. khandae*. *A. gobiensis* is similar to *A. minutus* in that the protoloph II are present on

M1-2. However, there are also distinct differences between the two taxa. In the new specimens, the mesoloph in M1-2 are shorter and the mesoconid is more distinct than that in *A. minutus*. *A. gobiensis* is larger than *A. minutus*.

A. gobiensis is more similar to *A. diconjugatus* from the Yuanqu Basin than other species of *Allosminthus*. However, *A. gobiensis* differs from *A. diconjugatus* in several aspects of the cheek teeth, including a more complete protoloph II on M1-2 that enclosed a deep fossette between the protocone and paracone, a weaker mesocone and a longer mesoloph, and more developed metalophid on m2 that is connected to the anterolophid. *Allosminthus* cf. *A. diconjugatus* was described based on specimens from the Houldjin Formation of Erenhot (Wang, 2008a), and the “Upper Red” beds from the Erden Obo section (Li, Q. et al., 2017). The differences mentioned above are also visible between *Allosminthus* cf. *A. diconjugatus* and *A. diconjugatus*. As the number of specimen increases, the differences between them are stable and distinct, so these characteristics justify the attribution of the new specimens to *Allosminthus gobiensis* n. sp. (see Table 1).

Allosminthus cf. *A. majusculus* Wang, 1985
(Fig. 5)

Specimens: Right M1 (IVPP V 25040.1), left m1 (IVPP V 25040.2), left m2 (IVPP V 25040.3), and right m2 (IVPP V 25040.4).

Locality and horizon: Erden Obo, Nomogen, Siziwangqi, Nei Mongol, China; “Middle Red” beds.

Description and comparisons: The anterior arm of the protocone on M1 is complete and extends labially to connect the anterior part to the protocone (Fig. 5A). The protoloph II is absent. The metaloph connects to the anterior arm of the hypocone. A distinct mesocone is present, but the mesoloph is weak. The entoloph is complete and joins the protocone.

The anteroconid is distinct on m1, and it is isolated. The protoconid and metaconid are connected by the posterior arm of the protoconid. The hypolophid joins the anterior arm of the hypoconid. The mesolophid and ectomesolophid are long (Fig. 5B). The ectolophid is short and not extended to the protoconid.

The anterolophid of m2 is developed (Fig. 5C, D). The short anterior arm of the protoconid and the metalophid are extended to the anterolophid. The posterior arm of the protoconid joins the metaconid and the trigonid is closed. The mesolophid is middle length and shorted than that in m1. The ectolophid is complete and longer than that in m1. The hypolophid is connected to the hypoconid.

Allosminthus majusculus was described based on the materials from the Qujing (Wang, 1985) and the Huoldjin Formation of Erenhot (Wang, 2008a). Compared to these specimens, the new materials from the "Middle Red" beds of the Erden Obo have a long mesolophid and ectomesolophid on m1. Based on these features, they are closer to the m1 of *Allosminthus* cf. *A. majusculus* from the "Upper Red" beds of the Erden Obo (Li, Q. et al., 2017). Their size is also comparable (see Table 2). The four molars are thus referred to *Allosminthus* cf. *A. majusculus*.

Allosminthus ernos Wang, 1985
(Fig. 6)

Specimens: Left mandible with m1-3 (IVPP V 25041.1), right m1 (IVPP V 25041.2), left m2 (IVPP V 25041.3), and right m3 (IVPP V 25041.4).

Locality and horizon: Erden Obo, Nomogen, Siziwangqi, Nei Mongol, China; "Middle Red" beds.

Description and comparisons: The anteroconid of m1 is small and isolated (Fig. 6A, B). The protoconid and metaconid are directly connected by the posterior arm of the protoconid. The mesoconid is distinct on the low ectolophid. The hypolophid is complete and extends to the hypoconid. The mesolophid is absent.

The m2 anterior arm of the protoconid is short and joins the anterolophid. The metalophid is weak (IVPP V 25041.1) (Fig. 6A), or short and extends to the anterior arm of the protoconid (IVPP V 25041.3) (Fig. 6C). Other characters are similar to those in m1.

The m3 anterior arm of the protoconid and the metalophid are connected by the anterolophid. The posterior arm of the protoconid is absent (IVPP V 25041.1) (Fig. 6A) or complete (IVPP V 25041.4) (Fig. 6D). The hypolophid is also absent (IVPP V 25041.1) (Fig. 6A) or extends to the anterior arm of the hypoconid (IVPP V 25041.4) (Fig. 6D).

The new specimens from the “Middle Red” beds of the Erden Obo have a complete posterior arm of the protoconid on m1-2, a varied metalophid on m2 and a varied posterior arm of the protoconid and hypolophid on m3, and have no mesolophid on m1-3. All the features are identical with those of *Allosminthus ernos*. The size of the new specimens falls within the range of variation of *A. ernos* (Wang, 1985; Li, Q. et al., 2017) (see Table 3).

Sinosminthus Wang, 1985

Sinosminthus sp.
(Fig. 3C)

Specimen: Left M1 (IVPP V 25042).

Locality and horizon: Erden Obo, Nomogen, Siziwangqi, Nei Mongol, China; “Middle White” beds.

Description and comparisons: This tooth measures (length/width in mm) 1.87/1.9. A small interdental wear facet is present on the anterior wall of the tooth. The four main cusps are robust and the crests are short and low. The double connection is present between the protocone and the paracone. The protoloph II is lower than the anterior arm of the protocone. The metaloph is short, and extends to the hypocone, but does not connect with the latter one. The mesoloph is long and reaches the labial border of the tooth.

Wang (1985) described *Sinosminthus inapertus* from Qujing. The new specimen from the “Middle White” beds is similar to *S. inapertus* in having complete anterior arm of the protocone and protoloph II between the protocone and paracone, the backward metaloph that not joins the hypocone, and long mesoloph. The M1 reported here is larger than that of *S. inapertus*. Recently, some specimens of *Sinosminthus* sp. from the "Upper Red" beds of the Erden Obo were reported (Li, Q. et al., 2017). These "Upper Red" beds specimens are similar to *S. inapertus*, except for larger size. M1 of *Sinosminthus* sp. is not found from the "Upper Red" beds, but the size of the specimens of *Sinosminthus* in "Middle White" and "Upper Red" beds is same, so here we refer the M1 from the "Middle White" beds to *Sinosminthus* sp. of the "Upper Red" beds.

Cricetidae Fischer de Waldheim

Cricetops Matthew and Granger, 1923

Cricetops dormitor Matthew and Granger, 1923

(Fig. 7)

Specimens: Right mandible with m1-3 (IVPP V 25043.1), right mandible with m2-3 (IVPP V 25043.2), and left mandible with m3 (IVPP V 25043.3).

Locality and horizon: Erden Obo, Nomogen, Siziwangqi, Nei Mongol, China; "Upper White" beds.

Description and comparisons: The mandible is a slender, with a long, weakly curved ventral edge of the mandible (Fig. 7A-C). The masseter crests are "V"-shaped (Fig. 7C); both the dorsal and the ventral crests are strong. The dorsal masseter crest joins the ventral one at a point below the middle of m2. The angular process lies in the same plane as the cheek teeth and incisor, so that the mandible is typical of sciurognathy.

A rudimentary anteroconid of m1 is weak and undivided, and much smaller than the other four cusps that arranged in two cusps pairs. The protoconid and hypoconid are crescentic, and they are located more distally relative to round metaconid and entoconid, respectively. The anterolophulid and the metalophulid connect directly to the anteroconid. The protoconid posterior arm is complete and connected to the base of the metaconid. The ectolophid is very short and oblique, a small mesoconid is present. The short hypolophid is oriented mesially, and connects directly to the mesoconid. The posterolophid is well developed, extends to the base of the entoconid, and delimits a large posterosinusid. There are no mesolophid, hypoconid posterior arm, and metaconid spur on m1.

The anteroconid is absent on m2 and m3 (Fig. 7D, E). The m2 metalophulid extends anterolabially to contact the anterolophulid. In m3, the metalophulid is connected to the lingual anterolophid, whereas the anterolophulid connects to the labial anterolophid. The protoconid posterior arm of m2-3 is longer than that in m1, and it meets the metaconid to close the trigonid basin on m2 or extends almost to the mesosinusid on m3. The mesoconid is small, the hypolophid connects to the mesoconid, and it is more transverse in m3 than that in m2. The mesosinusid is always open lingually, whereas labially the sinusid is usually closed by a cingulid. The m2-3 posterosinusid is noticeably large.

The new specimens from the Erden Obo have the brachyodont crowns in lower teeth. The cusps arrange in pairs. The outer cusps tend to be crescentic, and the inner cusps are nearly round. The mesolophid and ectomesolophid are absent on m1-3. All the features are identical with those of *Cricetops dormitor* (Matthew and Granger, 1923; Kowalski, 1974; Wang, 1987; Gomes Rodrigues et al., 2012). The size of the new specimens falls within the range of variation of *C. dormitor* (Kowalski, 1974) (see Table 4).

Eocricetodon Wang, 2007b

Eocricetodon sp.
(Fig. 8)

Specimens: Left M1 (IVPP V 25044.1-3), left M2 (IVPP V 25044.4), and right m2 (IVPP V 25044.5-7).

Locality and horizon: Erden Obo, Nomogen, Siziwangqi, Nei Mongol, China; “Middle Red” beds.

Description and comparisons: On M1 the anterior lobe is mid-sized with single anterocone. The main four cusps are massive and the lophs are short. The protocone spur extends to the anterocone (Fig. 8A). The protolophule is complete and connects the paracone and the posterior arm of the protocone. The metalophule is directed to the middle part of the hypocone. The mesoloph is usually long and reaches the labial border. On M2 the protolophule and metalophule join with the anterior arm of the protocone and the hypocone, respectively (Fig. 8B).

Both anterolophids of m2 are well developed, but the labial one is short. The metalophulid is long and extends anterolabially to contact the anterolophulid. The protoconid posterior arm is prominent, but it never meets the metaconid so that the trigonid basin is open posteriorly (Fig. 8C, D). The hypolophid is complete and is connected to the anterior arm of the hypoconid (2/3) or the hypoconid (1/3). The mesolophid is weak or short (Fig. 8C). A distinct mesoconid is present on the ectolophid.

The new specimens from the “Middle Red” beds of the Erden Obo have a single anterocone on the anterior lobe, a long protocone spur on M1 that connects to the anterocone, a complete protolophule on M1 that joins with the posterior arm of the protocone, and the metalophule on M1-2 extended to the anterior arm of the hypocone. All the features are identical with those of *Eocricetodon*. The new specimens differ from *Eocricetodon borealis* (Wang, 2008a) in having slightly larger size of M1-2 (see Table 5), and having no protoconule on M1 protocone spur and no mesolophid on m2. In *Eocricetodon meridionalis* (Wang and Meng, 1986; Wang, 2008a) the protoloph spur on M1 is occasionally short, but it is always long and extends to the anterocone in new specimens. The main cusps in upper molars of new specimens are more massive than those in *E. meridionalis*. Here these teeth are tentatively referred to *Eocricetodon*, but tentatively regarded as indeterminate at the specific level.

Eucricetodon Thaler, 1966

Eucricetodon cf. *E. wangae* Li, Meng, and Wang, 2016a

(Fig. 9)

Specimens: Right M1 (IVPP V 25045.1-2), and left m2 (IVPP V 25045.3).

Locality and horizon: Erden Obo, Nomogen, Siziwangqi, Nei Mongol, China; “Middle White” beds.

Description and comparisons: M1 bears a strong anterocone that located labial to the longitudinal axis of the tooth. The anterocone is transversely elongated and single lobed. The protocone spur is free and short, and the protolophule is complete and connects the paracone and the posterior side of the protocone (Fig. 9A). The metalophule is directed to the anterior part of the hypocone. The mesoloph is moderately elongated (Fig. 9B). The entoloph is long and extends obliquely, meeting the protolophule.

The metalophulid on m2 is long and extends anterolabially to contact the anterolophulid (Fig. 9C). The posterior arm of the protoconid is long and extends to the base of the metaconid. The hypolophid is complete and connected to the ectolophid. A short mesolophid is present.

The new specimens from the “Middle White” beds of the Erden Obo section are similar to *Eucricetodon wangae* (Li et al., 2016a) and *E. caducus* (Shevyreva, 1967; Wang, 1987) in having a short and free protocone spur on M1, the posterior connection of the protolophule and the anterior connection of the metalophule. The new specimens differ from *E. caducus* in lacking a close protosinus on M1, and having small size and a long protoconid posterior arm in m2. Compared to the holotype of *E. wangae*, the specimens reported here are slightly smaller (see Table 6), and the protocone spur is shorter. We regard the new specimens as *Eucricetodon* cf. *E. wangae*.

Pappocricetodon Tong, 1992

Pappocricetodon schaubi (Zdansky, 1930)
(Fig. 10)

Specimens: Right M1 (IVPP V 25046.1), and left M2 (IVPP V 25046.2).

Locality and horizon: Erden Obo, Nomogen, Siziwangqi, Nei Mongol, China; “Middle White” beds.

Description and comparisons: The teeth measurements (length/width in mm) are: 1.75/1.4 for M1 and 1.5/1.5 for M2. On M1 a small anterior lobe has a small anterocone. The protocone spur is long and reaches the distal base of the anterocone. From the lingual base of the paracone, the protolophule extends to the protocone spur (Fig. 10A). The metalophule is long and joins the anterior arm of the hypocone. The anterior arm of the hypocone is long and extending to the protolophule. The mesoloph is complete and reaches the labial border. The posterior arm of the protocone is absent. A small mesostyle is present.

M2 is square in occlusal view. The protolophule is complete and joins the anterior part of the protocone, and the metalophule joins the hypocone at its anterior side. The anterior arm of the hypocone is also long, and extends anteriorly to the central basin (Fig. 10B). The posterior arm of the protocone is absent. The mesoloph is moderately long.

The new specimens from the “Middle White” beds of the Erden Obo possess many characters common in *Pappocricetodon*, such as the brachyodont cheek teeth, a bulbous protocone in M1 and M2, a less enlarged M1 with small anterocone, and a long protocone spur extending to the anterocone. The anterocone on M1 of new specimens is larger than that in *P. neimongolensis* (Li, 2012), *P. antiquus* (Wang and Dawson, 1994), and *P. kazakstanicus* (Emry et al., 1998b). The protoconule on protolophule is present in *P. neimongolensis*, *P. antiquus*, and *P. kazakstanicus*, but it is absent in new M1. *P. siziwangqiensis* (Li et al., 2016a) differs from the new materials in having a short protolophule that joins the protocone on its posterior side. The size of the new specimens is similar to that of *P. schaubi* (Zdansky, 1930; Tong, 1997), but it is larger than that of *P. rencunensis* (Tong, 1992, 1997). The similar features and size shared by the new specimens and *P. schaubi* from the Yuanqu Basin.

5. Discussion and concluding remarks

5.1. “Upper White” beds

The “Upper White” beds were referred to the “Baron Sog” Formation by Osborn (1929), and they were called the “Upper Naogangdai” Formation by the geologists of

Nei Mongol (Jiang, 1983), which was adopted by Qiu and Wang (2007), and Wang et al. (2012). Wang (2003) suggested the age of the "Upper White" beds is early Oligocene, because it has been known to yield some mammalian fossils: *Paraceratherium grangeri*, *Entelodon gobiensis*, and *Schizotherium* cf. *S. avitum* (Coombs, 1978; Wang, 2003; Qiu and Wang, 2007), all of which are known to appear in early Oligocene.

Now, *Cricetops dormitor* is found from the "Upper White" beds. *Cricetops dormitor* occurred in a wide area of early Oligocene deposits in Mongolia (Matthew and Granger, 1923; Kowalski, 1974; Daxner-Höck et al., 2010), Kazakhstan (Shevyreva, 1965; Mellett, 1968; Emry et al., 1998a) and many localities in northern China (Wang, 1987; Gomes Rodrigues et al., 2012; Ye et al., 2005) (see Table 7). *Cricetops* is usually a dominant element in the early Oligocene faunas in North and Central Asia, and it is therefore widely regarded as an 'index taxon' of the early Oligocene in Asia (Matthew and Granger, 1923; Argyropulo, 1938; Shevyreva, 1967; Kowalski, 1974; Ni et al., 2007; Russell and Zhai, 1987; Wang, 1987). Moreover, *Cricetops dormitor* is an index fossil of the "*Cricetops dormitor* Taxon Range Zone" of the early Oligocene (range of biozones A+B) in the Valley of Lakes in Mongolia (Harzhauser et al., 2017). The materials of *Cricetops dormitor* from the Erden Obo confirm that the age of the "Upper White" beds is early Oligocene.

5.2. From "Middle Red" to "Upper Red" beds

Recently the ctenodactyloid fossils were described from the "Lower Red" to the "Upper Red" beds of the Erden Obo section (Li, in press). The dipodid and cricetid specimens from the "Upper Red" beds were also reported by Li. et al. (2016a) and Li, Q. et al. (2017). Here new dipodid and cricetid materials from the "Middle White" and "Middle Red" beds were recognized (Fig. 1). Now we present a rodent review from the "Middle Red" to "Upper Red" beds of Erden Obo section (see Table 7).

"Middle Red" beds:

Ctenodactyloidea: *Gobiomys neimongolensis*, *Gobiomys exiguus*

Cricetidae: *Eocricetodon* sp.

Dipodidae: *Allosminthus ernos*, *Allosminthus gobiensis*, *Allosminthus* cf. *A. majusculus*

"Middle White" beds:

Ctenodactyloidea: *Gobiomys neimongolensis*

Cricetidae: *Eucricetodon* cf. *E. wangae*, *Pappocricetodon schaubi*

Dipodidae: *Allosminthus gobiensis*, *Sinosminthus* sp.

"Upper Red" beds:

Ctenodactyloidea: *Gobiomys neimongolensis*, *Gobiomys exiguus*

Cricetidae: *Eucricetodon wangae*, *Eucricetodon* sp., *Pappocricetodon siziwangqiensis*

Dipodidae: *Allosminthus ernos*, *Allosminthus gobiensis*, *Allosminthus* cf. *A. majusculus*, *Sinosminthus* sp.

The ctenodactyloid and dipodid rodents from the "Middle Red" to the "Upper Red" beds of Erden Obo are very similar. They share *Gobiomys neimongolensis*, *Gobiomys exiguus*, *Allosminthus ernos*, *Allosminthus gobiensis*, *Allosminthus* cf. *A. majusculus*, *Sinosminthus* sp. Similarity, *Gobiomys neimongolensis* and *Gobiomys exiguus* were also found in the Houldjin Formation of Erenhot (Wang, 2001). Later, Wang (2008a) described the dipodids from the Houldjin Formation including *Allosminthus majusculus*, *Allosminthus gobiensis*, and *Allosminthus ernos*. The dipodids *Heosminthus primiveris*, *Sinosminthus inapertus*, *Allosminthus ernos*, *Allosminthus majusculus*, and *Allosminthus* sp. from the lower part of the Caijiachong Formation of the Qujing Basin, Yunnan were reported (Wang, 1985; Li, L.Z. et al., 2017). Obviously, the dipodids from the Houldjin Formation and the lower part of the Caijiachong Formation are similar to those from the "Middle Red" to the "Upper Red" beds (see Table 7).

However, the cricetid rodents from the "Middle Red" to the "Upper Red" beds are different, and the cricetids of the "Middle White" and "Upper Red" beds are different from those of the Houldjin Formation (*Eocricetodon borealis* and *Oxynocricetodon erenensis*) and the lower part of the Caijiachong Formation (*Eocricetodon meridionalis* and *Oxynocricetodon leptaleos*) (see Table 7). Based on the evolutionary trends of the early cricetids (Tong, 1992; Wang, 2007b), *Eucricetodon wangae* from the "Upper Red" beds of Erden Obo is more advanced than *Eocricetodon* and *Oxynocricetodon* from the Houldjin Formation and lower part of the Caijiachong Formation. *Pappocricetodon siziwangqiensis* of the "Upper Red" beds is more advanced than *Pappocricetodon* *schaubi* from the "Middle White" beds. *Pappocricetodon schaubi* that appears in "Middle White" beds is a common taxon in the Zhaili fauna of the Yuanqu Basin, Shanxi, and the age of Zhaili fauna is comparable to the Duchesnean of North America Land Mammal Age (Tong, 1997).

Based on the similar ctenodactyloids and dipodids from the "Middle Red" to the "Upper Red" beds of Erden Obo, Houldjin Formation and lower part of the Caijiachong Formation, the age of these beds is suggested to be contemporary. However, the cricetids from "Upper Red" beds is advanced than that from the "Middle White" beds or Houldjin Formation and lower part of the Chaijiachong Formation. *Eocricetodon* is present in "Middle Red" beds, Houldjin Formation and lower part of the Chaijiachong Formation. So, the age of the "Middle Red" and "Middle White" beds is probable more similar to the age of Late Eocene Houldjin Formation and lower part of the Chaijiachong Formation, and the age of "Upper Red" beds is younger than the these beds and it is probably close to the Eocene/Oligocene boundary.

The fauna associated with the rodent described here include abundant perissodactyls. The base of the "Middle Red" beds yielded remains of three perissodactyls, *Teleolophus magnum*, *Amynodontopsis parvidens*, and *Embolotherium grangeri* (Osborn, 1929; Radinsky, 1965; Mihlbachler, 2008). The latter two species were also known from the base of the Ula Gochu Formation at Baron Sog Mesa. The "Middle White" has relatively diverse perissodactyl fossils, bearing *Ardynia praecox* (Radinsky, 1967; Bai et al., 2018), *Proeggysodon qiui* (Bai and Wang, 2012), *Urtinotherium intermedium* (Chow and Qiu, 1963; Qiu and Wang, 2007), *Zaisanamynodon borisovi* (Lucas et al., 1996), *Embolotherium andrewsi*, and *Parabrontops gobiensis* (Osborn, 1929; Granger and Gregory, 1943; Mihlbachler, 2008). *Z. borisovi* and *E. andrewsi* were also known from the Barson Sog Formation at Baron Sog Mesa (Granger and Gregory, 1943; Lucas, et al., 1996; Mihlbachler, 2008). The time horizon of *Ardynia praecox* was confined to the late Eocene, most probably the latest Eocene Ergilian (Bai et al., 2018). *Proeggysodon qiui* is obviously younger than the Sharamurunian. Only chalicothere *Schizotherium* cf. *S. avitum* is known from "Upper Red" (Coombs, 1978). These perissodactyl taxa indicated that the age from the

“Middle Red” to “Upper Red” bed is most likely late Eocene.

5.3. “Lower Red” beds

In this horizon the ctenodactyloids *Gobiomys exiguus*, *Gobiomys neimongolensis* and *Yuomys magnus* were reported (Li, in press), and these mammal taxa indicate that the “Lower Red” beds are most likely late Middle Eocene. Here the dipodids *Primisminthus shanghenus* and *Allosminthus uniconjugatus* were described, and they are also found from the lower fossiliferous beds of the Rencun Member of the Hedi Formation of Shanghe, Henan (Tong, 1997; Wang, 2008a). Based on the small mammal fossils from Shanghe, the age of the Shanghe fauna is basically equivalent to the Sharamurunian of Asian Land Mammal Age and the late Uintan of North America Land Mammal Age. Our recent fieldworks discovered *Caenolophus promissus* and *Teilhardia pretiosa* from “Lower Red”. The type specimen of *C. promissus* was known from the Shara Murun Formation (Matthew and Granger, 1925). In addition to perissodactyl fossils, the “Lower Red” bed bears lagomorph *Gobiolagus aliwusuensis* that is considered to be Sharamurnian (Fostowicz-Frelik et al., 2012) and a molar of basal Glires taxon *Mimolagus actually* (Fostowicz-Frelik et al., 2015). As stated above, these mammal taxa form the “Lower Red” beds show that the age of this horizon is correlative to the Sharamurunian.

5.4. “Lower White” beds

The various small mammalian fossils have been reported from the “Lower White”, including rodent *Gobiomys exiguus*, *G. asiaticus* (Wang, 2001), *Pappocricetodon antiquus*, *P*. sp., *P*.? sp. (Wang, 2007b), lagomorph *Desmatolagus vetustus* (Wang, 2007a), primate *Eosimias* sp. (Wang, 2008b), insectivore *Anatolechinos neimongolensis*, Erinaceidae gen. et sp. indet., and chiroptere Microchiroptera gen. et sp. indet. (Wang, 2008c). However, we did not find rodent fossils in field expeditions in recent years. More attention should be paid to this horizon in the future work. *Pappocricetodon antiquus* from this horizon is more advanced than *Pappocricetodon neimongolensis* (Li, 2012) from the “Basal White” beds, and it is more primitive than

Pappocricetodon schaubi from the “Middle White” beds. *Gobiomys exiguus* are also found in the “Lower Red”, “Middle Red” and “Upper Red” beds (Li, in press). Therefore, the evolutionary level of the rodents from the “Lower White” beds reported by Wang (2001, 2007b) conforms to the evolution trend of rodents in the stratigraphic sequence.

5.5. Transformation of rodent assemblages

In the “Basal Red” beds of the Erden Obo section some rodent specimens were found that were included to Alagomyidae and Ctenodactyloidea; Ctenodactyloids are highly diversified in the lower part of the “Basal White” (Li et al., 2018) (see Table 8; Fig. 11), but declined from the “Lower White” beds (Fig. 11). Cricetids and dipodids are initially found in the middle part of “Basal White” beds of Irdinmanhan and the “Lower Red” beds of Sharamurunian, respectively (Fig. 1). During Late Eocene the diversity of cricetids and dipodids in the “Middle Red”, “Middle White” and “Upper Red” beds increased (Fig. 11). Based on the MNI (minimum number of individuals), it is evident that the rodent assemblages of the Erden Obo section show a transformation from ctenodactyloid dominant in early–middle Eocene to cricetid-dipodid dominant in late Eocene (see Table 8). Similarity, the biotic changes occurring at the end of the middle Eocene are also present in the Wulanhuxiu section in the Erlian Basin (Li et al., 2016b) , and in Liguanqiao and Yuanqu Basin (Tong, 1997). The faunal turnover probably responded to the environmental and climate changes.

Acknowledgements

I thank Bin Bai, Xun Jin, Ping Li, Jin Meng, K.C. Beard, D.L. Gebo, Xi-Jun Ni, Wei Chen, Wei Zhou, She-Jie Li, Qiang Cao, Wei Gao, Chen-Kai Sun, Hai-Bin Wang, Fang-Yuan Mao, Yong-Xin Wang, and Qi Li for assistance in fieldwork, and Yong-Fu Wang for specimen preparation. Hong-Wei Si for assistance in SEM. I thank Dr. Gudrun Daxner-Höck and an anonymous reviewer for constructive and critical reviews that improved the original manuscript. This research was supported by the Strategic Priority

Research Program of Chinese Academy of Sciences (XDB26000000), the National Natural Science Foundation of China (41572013). The fieldwork was also supported by the special Fund for Fossil Excavation and Preparation, CAS.

References

Argyropulo, A.I., 1938. On the fauna of Tertiary Cricetidae of the USSR. Compte Rendu (Doklady) de l'Académie des Sciences de l'URSS 20, 223–226.

Bai, B., Wang, Y.Q., 2012. *Proeggysodon* gen. nov., a primitive Eocene eggysodontine (Mammalia, Perissodactyla) from Erden Obo, Siziwangqi, Nei Mongol, China. Vertebrata PalAsiatica 50 (3), 204–218.

Bai, B., Wang, Y.Q., Zhang Z.Q., 2018. The late Eocene hyracodontid perissodactyl Ardynia from Saint Jacques, Inner Mongolia, China and its implications for the potential Eocene–Oligocene boundary. Palaeoworld 27, 247–257.

Chang, H.C., 1931. A brief summary of the Tertiary formations of Inner Mongolia and their correlation with Europe and North American. Bulletin of the Geological Society of China 10, 301–316.

Chow, M.C., Qiu, Z.X., 1963. New genus of giant rhinoceros from Oligocene of Inner Mongolia. Vertebrata PalAsiatica 7 (3), 230–239.

Chow, M.C., Rozhdestvensky, A.K., 1960. Exploration in Inner Mongolia a preliminary account of the 1959 field work of the Sino-Soviet Paleontological Expedition (SSPE). Vertebrata PalAsiatica 4 (1), 1–10.

Coombs, M.C., 1978. Additional *Schizotherium* material from China, and a review of *Schizotherium* dentitions (Perissodactya, Chalicotheriidae). American Museum Novitates 2647, 1–18.

Daxner-Höck, G., 2001. New zapodids (Rodentia) from Oligocene–Miocene deposits in Mongolia. Part 1. Senckenbergiana Lethaea 81 (1), 359–389.

Daxner-Höck, G., Badamgarav, D., Erbajeva, M., 2010. Oligocene stratigraphy based on a sediment-basalt association in central Mongolia (Taatsiin Gol and Taatsiin Tsagaan Nuur Area, Valley of Lakes): review of a Mongolian-Austrian project.

Vertebrata PalAsiatica 48 (4), 348–366.

Daxner-Höck, G., Badamgarav, D., Maridet, O., 2014. Dipodidae (Rodentia, Mammalia) from the Oligocene and Early Miocene of Mongolia. Annalen des Naturhistorischen Museums in Wien, Serie A116, 131–214.

Emry, R.J., Lucas, S.G., Tyutkova, L.A., Wang, B.Y., 1998a. The Ergilian–Shandgolian (Eocene–Oligocene) transition in the Zaysan Basin, Kazakstan. Bulletin of Carnegie Museum of Natural History 34, 298–312.

Emry, R.J., Tyutkova, L.A., Lucas, S.G., Wang, B.Y., 1998b. Rodents of the Middle Eocene Shinzhaly fauna of eastern Kazakhstan. Journal of Vertebrate Paleontology 18 (1), 218–227.

Fostowicz-Frelik, Ł., Li, C.K., Meng, J., Wang, Y.Q., 2012. New *Gobiolagus* (Mammalia: Lagomorpha) material from the Middle Eocene of Erden Obo (Nei Mongol, China). Vertebrata PalAsiatica 50 (3), 219–236.

Fostowicz-Frelik, Ł., Li, C.K., Mao, F.Y., Meng, J., Wang, Y.Q., 2015. A large mimotonid from the Middle Eocene of China sheds light on the evolution of lagomorphs and their kin. Scientific Reports 5, 9394, doi: 10.1038/srep09394.

Gomes Rodrigues, H., Marivaux, L., Viaeny-Liaud, M., 2012. The Cricetidae (Rodentia, Mammalia) from the Ulantatal area (Inner Mongolia, China): New data concerning the evolution of Asian cricetids during the Oligocene. Journal of Asian Earth Sciences 56, 160–179.

Granger, W., 1928. Records of fossils, Mongolia 1928. Third Central Asiatic Expeditions (Field Notes). American Museum of Natural History, New York, 79 pp.

Granger, W., Gregory, W.K., 1943. A revision of the Mongolian titanotheres. Bulletin of American Museum of Natural History 80 (10), 349–389.

Harzhauser, M., Daxner-Höck, G., Erbajeva, M.A., López-Guerrero, P., Maridet, O., Oliver, A., Piller, W. E., Göhlich, U.B., Ziegler, R., 2017. Oligocene and early Miocene mammal biostratigraphy of the Valley of Lakes in Mongolia. Palaeobiodiversity and Palaeoenvironments 97 (1), 219–231.

Jiang, H.X., 1983. Division of the Paleogene in the Erlian Basin of Inner Mongolia.

Geology of Inner Mongolia 2, 18–36 (in Chinese).

Kowalski, K., 1974. Middle Oligocene rodents from Mongolia. Palaeontologia Polonica 30, 147–178.

Li, L.Z., Ni, X.J., Lu, X.Y., Li, Q., 2017. First record of *Cricetops* rodent in the Oligocene of southwestern China. Historical Biology 29 (4), 488–494.

Li, Q., 2012. Middle Eocene cricetids (Rodentia, Mammalia) from the Erlian Basin, Nei Mongol, China. Vertebrata PalAsiatica 50 (3), 237–244.

Li, Q., in press. Eocene ctenodactyloid rodent assemblages and diversification from Erden Obo, Nei Mongol, China. Historical Biology, doi: 10.1080/08912963.2017.1395422.

Li, Q., Meng, J., Wang, Y.Q., 2016a. New cricetid rodents from strata near the Eocene–Oligocene boundary in Erdent Obo Section (Nei Mongol, China). PLOS ONE 11 (5), e0156233, doi: 10.1371/journal.pone.0156233.

Li, Q., Wang, Y.Q., Fostowicz-Frelik, Ł., 2016b. Small mammal fauna from Wulanhuxiu (Nei Mongol, China) implies the Irdinmanhan–Sharamurunian (Eocene) faunal turnover. Acta Palaeontologica Polonica 61 (4), 759–776.

Li, Q., Gong, Y.X., Wang, Y.Q., 2017. New dipodid rodents from the Late Eocene of Erden Obo (Nei Mongol, China). Historical Biology 29 (5), 692–703.

Li, Q., Mao, F.Y., Wang, Y.Q., 2018. First record of Eocene fossil rodent assemblages from the lower part of the Erden Obo Section, Erlian Basin (Nei Mongol, China) and its biochronological implications. Palaeobiodiversity and Palaeoenvironments 98 (2), 259–276.

Lucas, S.G., Emry, R.J., Bayshashov, B.U., 1996. *Zaisanamynodon*, a Late Eocene amynodontid (Mammalia, Perissodactyla) from Kazakhstan and China. Tertiary Research 17, 51–58.

Maridet, O., Ni, X.J., 2013. A new cricetid rodent from the early Oligocene of Yunnan, China, and its evolutionary implications for early Eurasian cricetids. Journal of Vertebrate Paleontology 3665, 1–21.

Matthew, W.D., Granger, W., 1923. Nine new rodents from the Oligocene of Mongolia. American Museum Novitates 102, 1–10.

Matthew, W.D., Granger, W., 1925. New mammals from the Shara Murun Eocene of Mongolia. American Museum Novitates 196, 1–12.

Mellett, J.S., 1968. The Oligocene Hsanda Gol Formation, Mongolia: a revised faunal list. American Museum Novitates 2318, 1–16.

Mihlbachler, M.C., 2008. Species taxonomy, phylogeny, and biogeography of the Brontotheriidae (Mammalia: Perissodactyla). Bulletin of the American Museum of Natural History 311, 1–475.

Ni, X.J., Meng, J., Wu, W.Y., Ye, J., 2007. A new Early Oligocene peradectine marsupial (Mammalia) from the Burqin region of Xinjiang, China. Naturwissenschaften 94, 237–241.

Osborn, H.F., 1929. *Embolotherium*, gen. nov., of the Ulan Gochu, Mongolia. American Museum Novitates 353, 1–20.

Pei, W.Z., Chow, M.C., Zheng, J.J., 1963. The Chinese Cenozoic Erathem. Science Press, Beijing, 31 pp.

Qi, T., 1990. A Paleogene section at Erden Obo, Nei Mongol and on the discovery of *Pastoralodon lacustris* (Pantodonta, Mammalia) in that area. Vertebrata PalAsiatica 28 (1), 25–33 (in Chinese, with English abstract).

Qiu, Z.X., Wang, B.Y., 2007. Paracerathere fossils of China. Palaeontologia Sinica, New Series C 29, 1–396.

Radinsky, L.B., 1964. Notes on Eocene and Oligocene fossil localities in Inner Mongolia. American Museum Novitates 2180, 1–11.

Radinsky, L.B., 1965. Early Tertiary Tapiroidea of Asia. Bulletin of American Museum of Natural History 129 (2), 181–264.

Radinsky, L.B., 1967. A review of the rhinocerotoid family Hyracodontidae (Perissodactyla). Bulletin of the American Museum of Natural History 136 (1), 1–46.

Russell, D.E., Zhai, R.J., 1987. The Paleogene of Asia: mammals and stratigraphy. Sciences de la Terre Series C 52, 1–488.

Shevyreva, N.S., 1965. New Oligocene Hamster of USSR and Mongolia. Paleontological Journal 1, 105–114 (in Russian).

Shevyreva, N.S., 1967. Hamsters of the genus *Cricetodon* from the Middle Oligocene of Central Kazakhstan. Paleontological Journal 2, 90–98 (in Russian).

Thaler, L., 1966. Les rongeurs fossiles du Bas-Languedoc dans leurs rapports avec l'histoire des faunes et la stratigraphie du Tertiaire d'Europe. Mémoires du Muséum National d'Histoire Naturelle Série C Géologie 17, 1–295.

Tong, Y.S., 1992. *Pappocricetodon*, a pre-Oligocene cricetid genus (Rodentia) from central China. Vertebrata PalAsiatica 30 (1), 1–16 (in Chinese, with English abstract).

Tong, Y.S., 1997. Middle Eocene small mammals from Liguanqiao Basin of Henan Province and Yuanqu Basin of Shanxi Province, Central China. Palaeontologia Sinica, New Series C 26, 1–256.

Wang, B.Y., 1985. Zapodidae (Rodentia, Mammalia) from the Lower Oligocene of Qujing, Yunnan, China. Mainzer Geowissenschaftliche Mitteilungen 14, 345–367.

Wang, B.Y., 1987. Discovery of cricetids (Rodentia, Mammalia) from middle Oligocene of Nei Mongol, China. Vertebrata PalAsiatica 25 (1), 187–198 (in Chinese, with English abstract).

Wang, B.Y., 2001. Eocene ctenodactyloids (Rodentia, Mammalia) from Nei Mongol, China. Vertebrata PalAsiatica 39 (2), 98–114 (in Chinese, with English abstract).

Wang, B.Y., 2003. Oligocene rodents from the Nomogen (= Nom Khong) Area of Nei Mongol, China, and comments on related stratigraphy. Vertebrata PalAsiatica 41 (3), 211–219 (in Chinese, with English abstract).

Wang, B.Y., 2007a. Late Eocene lagomorphs from Nei Mongol, China. Vertebrata PalAsiatica 45 (1), 43–58 (in Chinese, with English abstract).

Wang, B.Y., 2007b. Late Eocene cricetids (Rodentia, Mammalia) from Nei Mongol, China. Vertebrata PalAsiatica 45 (3), 195–212 (in Chinese, with English abstract).

Wang, B.Y., 2008a. Additional rodent material from Houldjin Formation of Erenhot, Nei Mongol, China. Vertebrata PalAsiatica 46 (1), 2–30 (in Chinese, with English abstract).

Wang, B.Y., 2008b. First record of primate fossils from late Eocene in Eren Region, Nei Mongol, China. Vertebrata PalAsiatica 46 (2), 81–89 (in Chinese, with English abstract).

Wang, B.Y., 2008c. First record of Late Eocene insectivores and chiropteres from Nei Mongol, China. Vertebrata PalAsiatica 46 (4), 249–264 (in Chinese, with English abstract).

Wang, B.Y., 2009. On *Tatalsminthus* (Dipodidae, Rodentia). Vertebrata PalAsiatica 47 (1), 81–84 (in Chinese, with English abstract).

Wang, B.Y., Dawson, M.R., 1994. A primitive cricetid (Mammalia: Rodentia) from the Middle Eocene of Jiangsu Province, China. Annals of Carnegie Museum 63, 239–256.

Wang, B.Y., Meng, J., 1986. *Eucricetodon* (Rodentia, Mammalia) from the Lower Oligocene of Qujing, Yunnan, China. Vertebrata PalAsiatica 24 (2), 110–120 (in Chinese, with English abstract).

Wang, Y.Q., Meng, J., Jin, X., 2012. Comments on Paleogene localities and stratigraphy in the Erlian Basin, Nei Mongol, China. Vertebrata PalAsiatica 50 (3), 181–203 (in Chinese, with English abstract).

Ye, J., Meng, J., Wu, W.Y., Ni, X.J., 2005. Late Eocene–Early Oligocene lithological and biological stratigraphy in the Burqin region of Xinjiang. Vertebrata PalAsiatica 43 (1), 49–60 (in Chinese, with English abstract).

Zdansky, O., 1930. Die Alttertiaren Saugetiere Chinas nebst stratigraphischen Bemerkungen. Palaeontologia Sinica, New Series C 6, 1–87.

Fig. 1. Stratigraphic distribution of rodent taxa in the Erden Obo section, plotted on a section modified from Granger (1928). Note: The stratigraphic ranges of one species are drawn as lines between the first and last occurrence. Ctenodactyloids are figured as a black square, dipodids as a hollow square, cricetids as a black triangle, alagomyids as a black circle and ischyromyids as a hollow circle. The species figured in grey are from the previous studies (Wang, 2001, 2007a). ALMA is Asian Land Mammal Age.

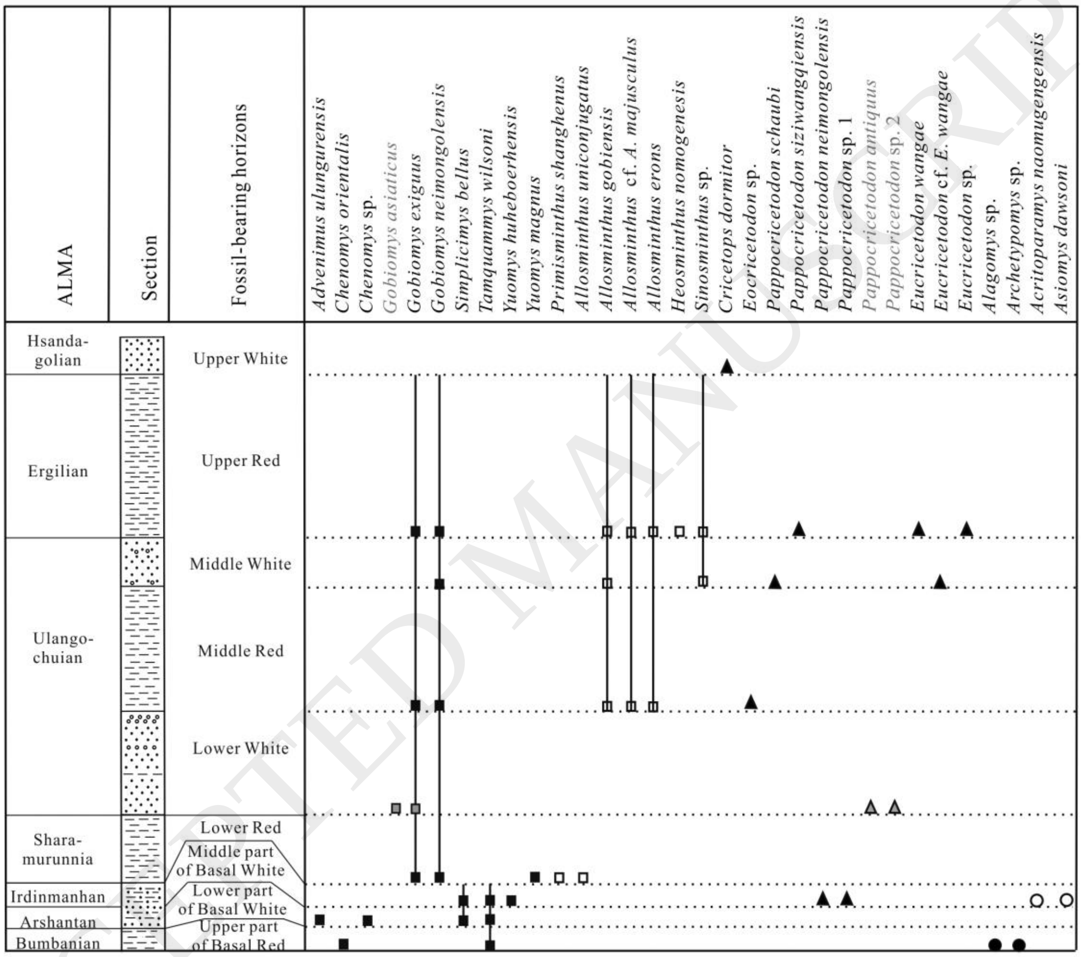

Fig. 2. Terminology used in this paper to described molars, modified from Li, Q. et al. (2016a, 2017). (A) Dipodids upper molar: 1. paracone, 2. mesostyle, 3. mesoloph, 4. metacone, 5. metaloph, 6. posteroloph, 7. hypocone, 8. mesocone, 9. sinus, 10. entoloph, 11. protocone, 12. anterior arm of protocone, 13. protoloph II, 14. anterior cingulum, 15. lingual anteroloph, 16. Anterolophule, 17. protoloph I, 18. labial anteroloph; dipodids lower molar: 19. metaconid, 20. posterior arm of protoconid, 21. mesolophid, 22. entoconid, 23. posterolophid, 24. hypolophid, 25. hypoconulid, 26. hypoconid, 27.

ectolophid, 28. mesoconid, 29. protoconid, 30. anteroconid, 31. ectomesolophid, 32. labial anterolophid, 33. anterior arm of protoconid, 34. Metalophid, 35. lingual anterolophid. (B) Cricetids upper molar: 1. protocone spur, 2. paracone, 3. protolophule, 4. mesostyle, 5. metacone, 6. posteroloph, 7. metalophule, 8. hypocone, 9. sinus, 10. protocone, 11. anterocone, 12. mesoloph, 13. mesocone, 14. entoloph, 15. lingual anteroloph, 16. labial anteroloph; cricetids lower molar: 17. metaconid, 18. protoconid posterior arm, 19. mesolophid, 20. entoconid, 21. posterolophid, 22. hypolophid, 23. hypoconid, 24. mesoconid, 25. protoconid, 26. anteroconid, 27. anterolophulid, 28. labial anterolophid, 29. metalophulid, 30. lingual anterolophid.

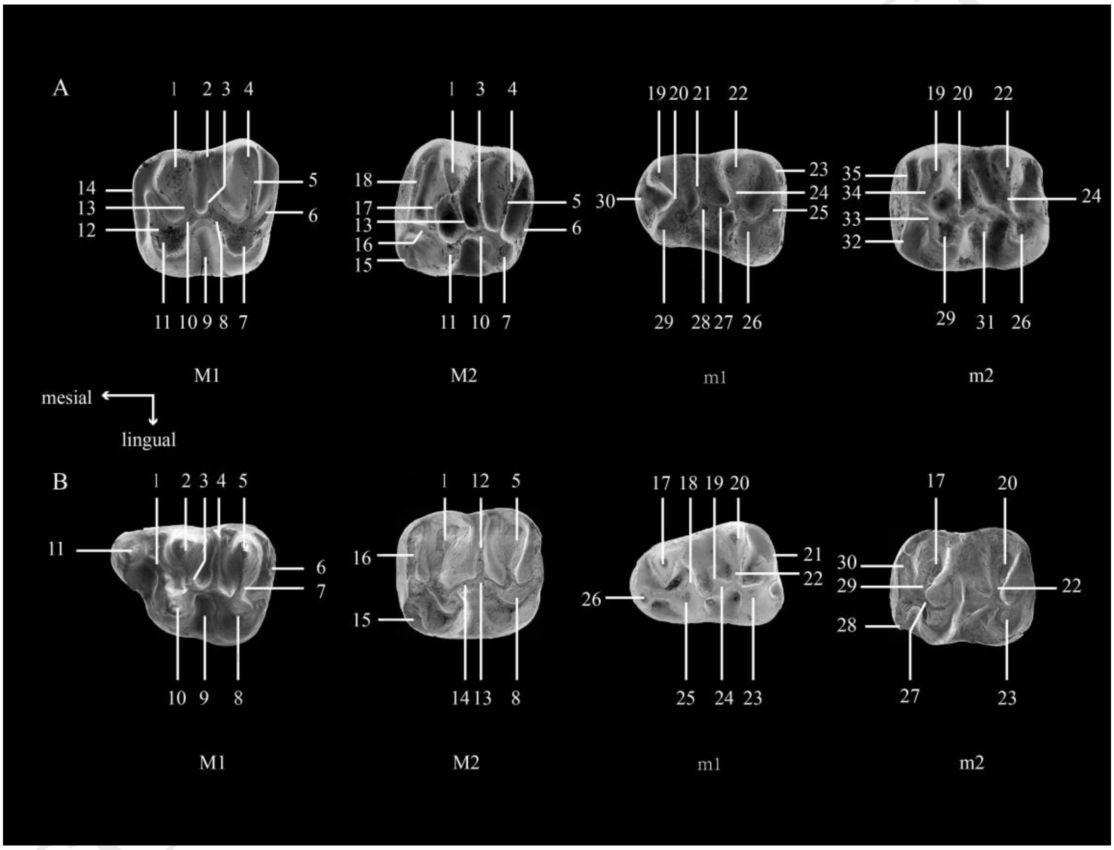

Fig. 3. (A) *Primisminthus shanghenus*, a left M1 (IVPP V 25036) in occlusal view. (B) *Allosminthus uniconjugatus*, a left M1 (IVPP V 20537) in occlusal view. (C) *Sinosminthus* sp., a left M1 (IVPP V 25042) in occlusal view. (A, B) at same scale.

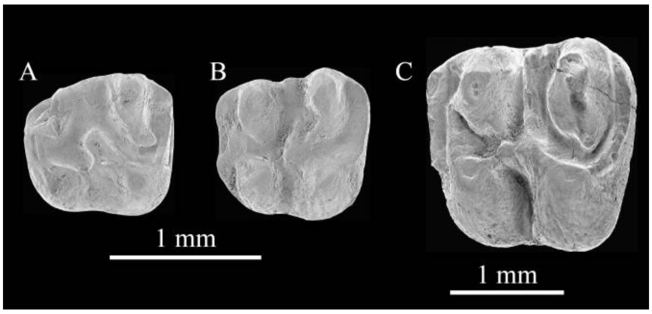

Fig. 4. Cheek teeth of *Allosminthus gobiensis* n. sp. (A) IVPP V 25038.1, right maxilla with broken P4-M1; (B, C) IVPP V 25038.2, occlusal and labial view of the right mandible with m1-3; (D) IVPP V 25039.1, left M1; (E) IVPP V 25039.1, left M2; (F) IVPP V 25039.9, right M2; (G) IVPP V 25039.10, left m1; (H) IVPP V 25038.5, left m1; (I) IVPP V 25038.6, left m2; (J) IVPP V 25039.17, right m2; (K) IVPP V 25039.19, left m3. (A, B, D-K) at same scale.

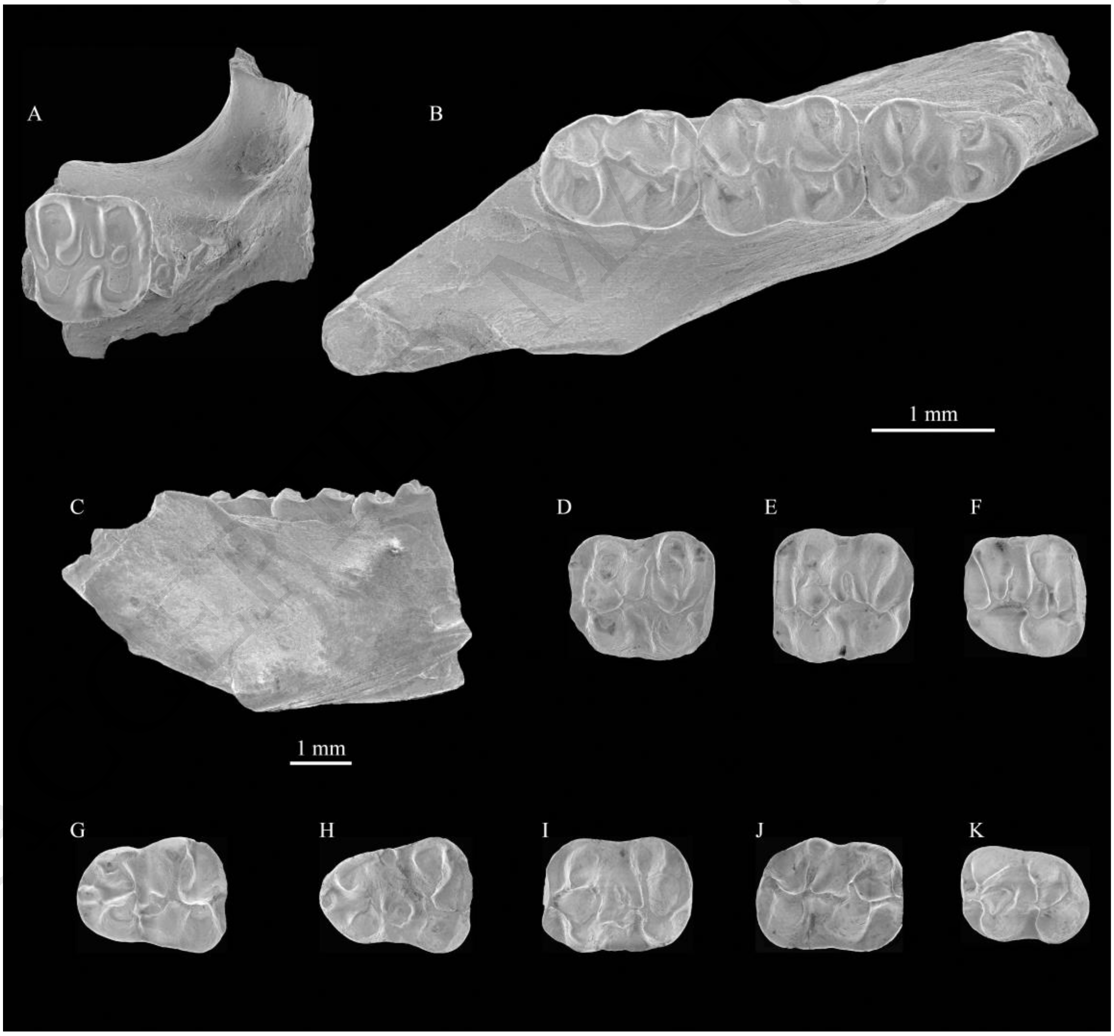

Fig. 5. Cheek teeth of *Allosminthus* cf. *A. majusculus* in occlusal view. (A) IVPP V 25040.1, right M1; (B) IVPP V 25040.2, left m1; (C) IVPP V 25040.3, left m2; (D)

IVPP V 25040.4, right m2.

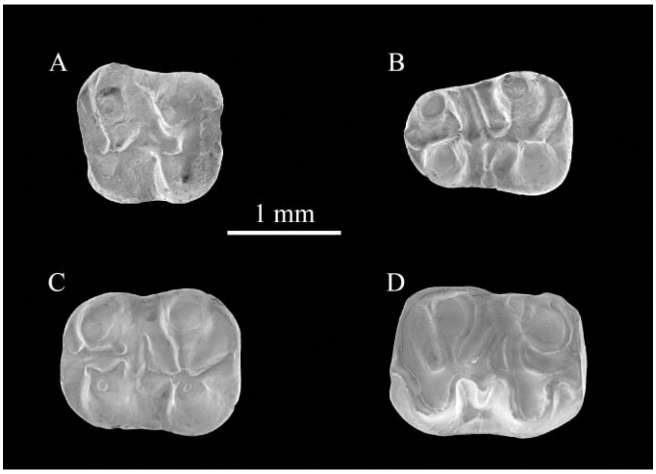

Fig. 6. Cheek teeth of *Allosminthus ernos* in occlusal view. (A) IVPP V 25041.1, left mandible with m1-3; (B) IVPP V 25041.2, right m1; (C) IVPP V 25041.3, left m2; (D) IVPP V 25041.4, right m3.

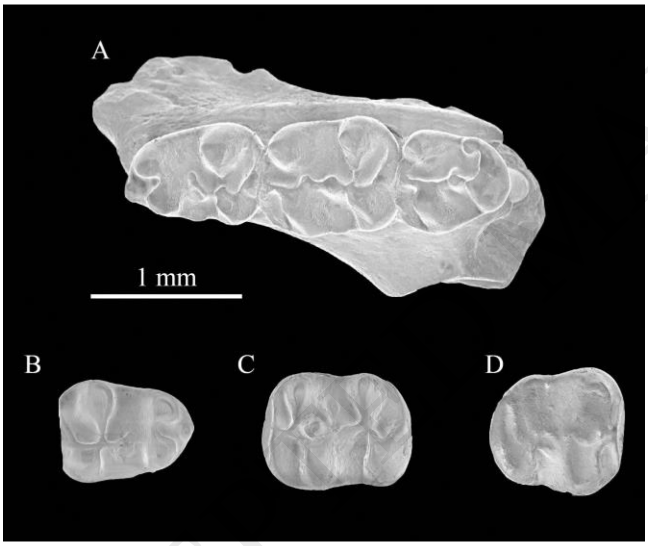

Fig. 7. Mandibles of *Cricetops dormitor*. (A-C) IVPP V 25043.1, occlusal, lingual and labial views of the right mandible with m1-3; (D) IVPP V 25043.2, occlusal view of the right mandible with m2-3; (E) IVPP V 25043.3, occlusal view of the left mandible with m3. (B, C) and (D, E) with same scale separately.

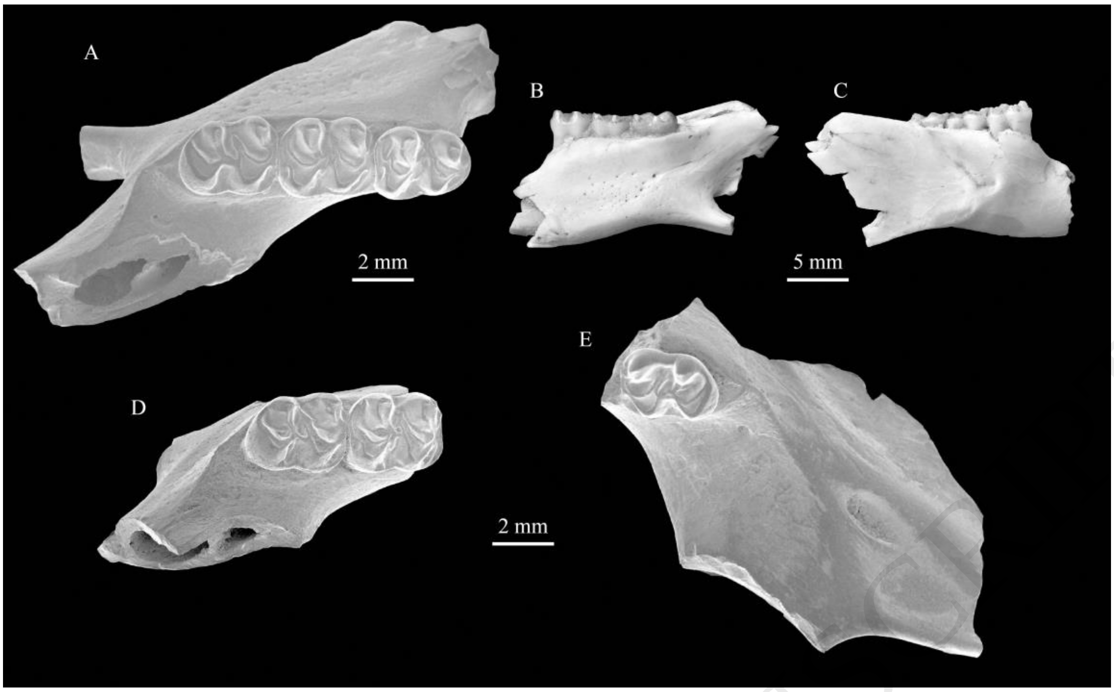

Fig. 8. Cheek teeth of *Eocricetodon* sp. in occlusal view. (A) IVPP V 25044.1, left M1; (B) IVPP V 25044.4, left M2; (C, D) IVPP V 25044.5-6, right m2.

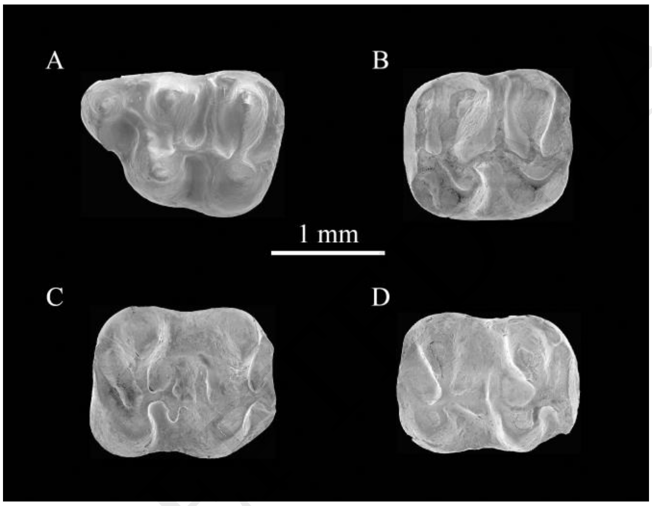

Fig. 9. Cheek teeth of *Eucricetodon* cf. *E. wangae* in occlusal view. (A) IVPP V 25045.1, right M1; (B) IVPP V 25045.2, right M1; (C) IVPP V 25045.3, left m2.

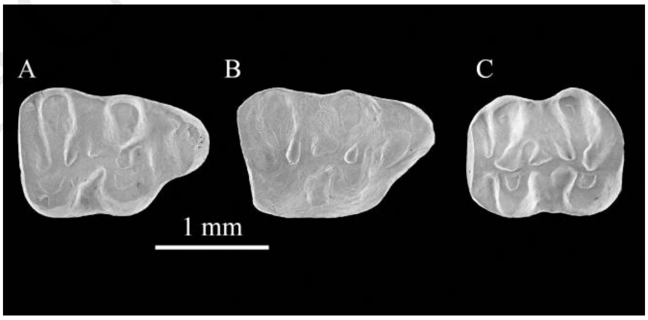

Fig. 10. Cheek teeth of *Pappocricetodon schaubi* in occlusal view. (A) IVPP V 25046.1,

right M1; (B) IVPP V 25046.2, left M2.

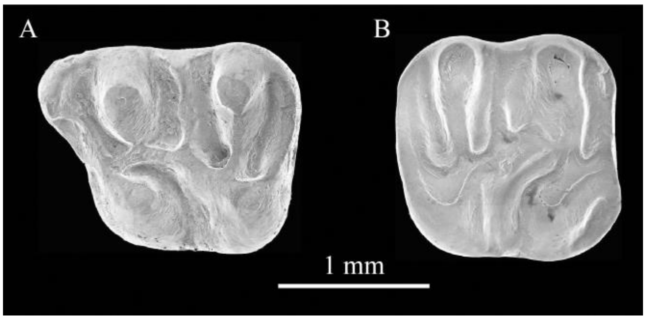

Fig. 11. The diversity of species of ctenodactyloids, cricetids, and dipodids from the Erden Obo section.

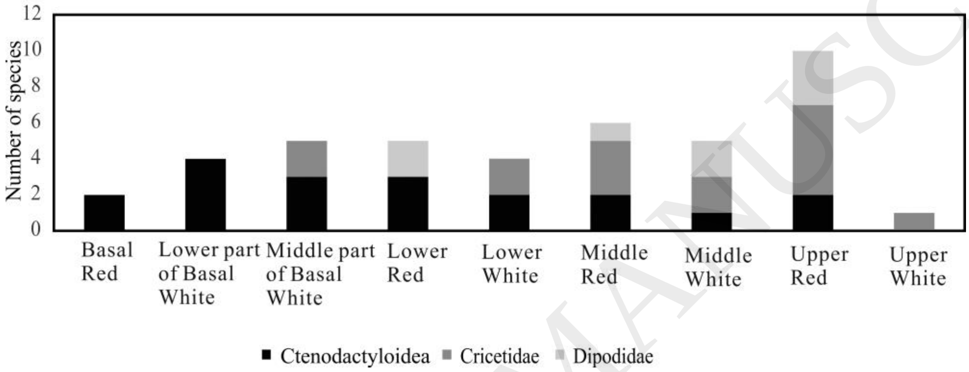

Table 1. Measurements of teeth of *Allosminthus gobiensis* n. sp. (mm).

	A. gobiensis (from Middle White and Middle Red beds of Erden Obo)			*A. gobiensis* (from Upper Red beds of Erden Obo) (Li, Q. et al., 2017)			*A. gobiensis* (from Erenhot) (Wang, 2008a)	
	number	range	mean	number	range	mean	number	range
M1 (L)	6	1.03-1.2	1.13	5	1-1.1	1.05	2	1.06-1.1
M1 (W)	6	1-1.18	1.06	5	0.95-1	1	3	1-0.9
M2 (L)	4	0.98-1.15	1.07					
M2 (W)	4	0.85-1.1	0.99					
M3 (L)							1	0.8
M3 (W)							1	0.9
m1 (L)	6	1.06-1.25	1.14	1	1.3	1.3	1	1.2
m1 (W)	6	0.78-1	0.91	1	1	1	3	0.9-0.95
m2 (L)	13	1.05-1.37	1.21	2	1.15-1.25	1.2	4	1.1-1.35
m2 (W)	13	0.8-1.13	0.99	2	0.95-1	0.98	4	0.9-1.1
m3 (L)	5	1-1.25	1.13					
m3 (W)	5	0.8-1.05	0.94					

Table 2. Measurements of teeth of *Allosminthus majusculus* (mm).

	Allosminthus cf. *A. majusculus* (from “Middle Red” beds)			*Allosminthus* cf. *A. majusculus* (from “Upper Red” beds) (Li, Q. et al., 2017)			*Allosminthus majusculus* (from Erenhot) (Wang, 2008a)	
	number	range	mean	number	range	mean	number	range
M1 (L)	1	1.3	1.3	8	1.35-1.55	1.47		
M1 (W)	3	1.25	1.25	8	1.25-1.5	1.41		
M2 (L)				7	1.25-1.55	1.39		
M2 (W)				7	1.3-1.45	1.36		
m1 (L)	1	1.5	1.5	6	1.5-1.65	1.6	2	1.4-1.6
m1 (W)	1	1.1	1.1	6	1.05-1.25	1.15	2	1.1
m2 (L)	2	1.6-1.75	1.68	8	1.5-1.75	1.63	1	1.45
m2 (W)	2	1.3-1.35	1.33	8	1.2-1.55	1.38	1	1.2

Table 3. Measurements of teeth of *Allosminthus ernos* (mm).

	A. ernos (Middle Red beds of Erden Obo)			*A. ernos* (Upper Red beds of Erden Obo) (Li, Q. et al., 2017)		*A. ernos* (from Qujing) (Wang, 1985)		*A. ernos* (from Erenhot) (Wang, 2008a)	
	number	range	mean	range	mean	range	mean	range	mean
m1 (L)	2	0.9-0.98	0.94	0.95-1.25	1.06	1-1.06	1.03		
m1 (W)	2	0.65-0.68	0.67	0.65-0.85	0.76	0.69-0.75	0.72		
m2 (L)	2	0.91-1	0.95	0.95-1.25	1.06	0.92-1.13	1.05	1.06	1.06
m2 (W)	2	0.9	0.9	0.8-0.95	0.89	0.67-0.88	0.81	0.76	0.76
m3 (L)	2	0.78-0.9	0.84	0.85	0.85	0.82	0.82		
m3 (W)	2	0.65-0.85	0.75	0.7-0.9	0.77	0.8	0.8		

Table 4. Measurements of teeth of *Cricetops dormitor* (mm).

	m1 (IVPP V 25043.1)	m2 (IVPP V 25043.1)	m3 (IVPP V 25043.1)	m2 (IVPP V 25043.2)	m3 (IVPP V 25043.2)	m3 (IVPP V 25043.3)
L	3.5	3.1	3	3.1	3	3.2
M	2.4	2.6	2.6	2.6	2.5	2.4

Table 5. Measurements of teeth of *Eocricetodon* (mm).

	Eocricetodon sp. (from Erden Obo)			*Eocricetodon meridionalis* (from Qujing) (Wang and Meng, 1986)			*Eocricetodon borealis* (from Erenhot) (Wang, 2008a)	
	number	range	mean	number	range	mean	number	range
M1(L)	1	1.8	1.8	4	1.64-1.84	1.74	3	1.6
M1(W)	3	1.2-1.4	1.32	9	1-1.31	1.19	4	1.04-1.15
M2 (L)	1	1.5	1.5	2	1.47-1.5	1.49	2	1.3-1.34
M2 (W)	1	1.35	1.35	3	1.18-1.34	1.24	2	1.18-1.3
m2 (L)	3	1.63-1.65	1.64	3	1.38-1.5	1.45	2	1.5-1.6
m2 (W)	3	1.25-1.35	1.3	6	1.13-1.25	1.21	2	1.2-1.25

Table 6. Measurements of teeth of *Eucricetodon wangae* (mm).

	Eucricetodon cf. *E. wangae*			*Eucricetodon wangae* (Li et al., 2016a)		
	number	range	mean	number	range	mean
M1 (L)	2	1.7-1.76	1.73	12	1.75-2.2	1.97
M1 (W)	2	1.15	1.15	12	1.3-1.5	1.38
m2 (L)	1	1.4	1.4	11	1.5-1.8	1.57
m2 (W)	1	1.15	1.15	11	1.15-1.4	1.28

Table 7. Comparison of rodent fossil assemblages from the “Middle Red” to “Upper White” beds of the Erden Obo with selected fauna in Asia.

Taxon	Locality and horizon						
	Middle Red, Erden Obo	Middle White, Erden Obo	Upper Red, Erden Obo	Upper White, Erden Obo	Houldjin Formation, Nei Mongol	Saint Jacques, Nei Mongol	Zaili, Yuanqu Shanxi
Ctenodactyloidea							
Gobiomys exiguus	√		√		√		
Gobiomys neimongolensis	√	√	√		√		
Karakoromys decessus							
Cricetidae							
Cricetops dormitor				√		√	
Cricetops auster							
Eocricetodon borealis					√		
Eocricetodon meridionalis							
Eocricetodon sp.	√						
Eucricetodon asiaticus							
Eucricetodon caducus						√	
Eucricetodon wangae			√				
Eucricetodon cf. *E. wangae*		√					
Eucricetodon sp.			√				
Oxynocricetodon erenensis					√		
Oxynocricetodon leptaleos							
Pappocricetodon schaubi		√					√
Pappocricetodon siziwangqiensis			√				
Paracricetops virgatoincisus							
Selenomys mimicus						√	
Ulaancricetodon badamae							
Ulaancricetodon cf. *U. badamae*							
Dipodidea							
Allosminthus diconjugatus							√
Allosminthus majusculus					√		
Allosminthus cf. *A. majusculus*	√		√				
Allosminthus ernos	√		√		√		
Allosminthus gobiensis	√	√	√		√		
Allosminthus khandae							
Allosminthus sp.							

Bohlinosminthus parvulus							
Heosminthus chimidae							
Heosminthus nomogenesis			√				
Heosminthus primiveris							
Heosminthus sp.							
Onjosminthus baindi							
Parasminthus							
Priminsminthus jinus							√
Shamosminthus sodovis							
Sinosmimthus inapertus							
Sinosminthus sp.		√	√				
Talasminthus							

Note: The rodent taxa of Erden Obo, Nei Mongol from Li, Q. et al. (2016a, 2017) and Li (in press); the taxa of Houldjin Formation, Nei Mongol from Wang (2001, 2007a, 2008a); the taxa of Saint Jacques, Nei Mongol from Wang (1987); the taxa of Zaili, Yuanqu, Shanxi from Tong (1997); the taxa of Caijiachong Formation, Yunan from Wang (1985), Li, L.Z. et al. (2017), and Maridet and Ni (2013); the taxa of Keziletuogaiyi Formation, Xinjiang from Ye et al. (2005); the taxa of Zaysan Basin, Kazakstan from Emry et al. (1998a); and the taxa of A biozone of Hsanda Gol and Loh Formation, Mongolia from Daxner-Höck et al. (2010).

Table 8. Relative abundance of rodents from the "Basal Red" to "Upper White" beds of the Erden Obo section. TNS: total number of specimens; MNI: minimum number of individuals; PEH: percent of the fauna of each horizon.

Horizon	**Taxa**	**Species**	**TNS**	**MNI**	**PEH**
Basal Red	Alagomyidae	*Alagomys* sp.	1	1	25%
		Archetypomys sp.	2	1	25%
	Ctenodactyloidea	*Chenomys orientalis*	1	1	25%
		Tamquammys wilsoni	2	1	25%
Lower part of Basal White	Ctenodactyloidea	*Advenimus ulungurensis*	3	1	6.67%
		Chenomys sp.	3	1	6.67%
		Simplicimys bellus	54	8	53.33%
		Tamquammys wilsoni	29	5	33.33%
Middle part of Basal White	Ctenodactyloidea	*Simplicimys bellus*	19	4	26.66%
		Tamquammys wilsoni	38	6	40%
		Yuomys huheboerhensis	3	1	6.67%
	Cricetidae	*Pappocricetodon neimongolensis*	1	1	6.67%
		Pappocricetodon sp.	1	1	6.67%
	Ischyromyidae	*Acritoparamys naomugengensis*	2	1	6.67%
		Asiomys dawsoni	3	1	6.67%
Lower Red	Ctenodactyloidea	*Gobiomys exiguus*	13	3	27.27%
		Gobiomys neimongolensis	1	1	9.09%
		Yuomys magnus	15	5	45.45%
	Dipodidae	*Allosminthus uniconjugatus*	1	1	9.09%
		Primisminthus shanghenus	1	1	9.09%
Lower White	Ctenodactyloidea	*Gobiomys exiguus*	5	2	33.33%
		Gobiomys asiaticus	5	2	33.33%
	Cricetidae	*Pappocricetodon antiquus*	5	1	16.67%
		Pappocricetodon sp.	1	1	16.67%
Middle Red	Ctenodactyloidea	*Gobiomys exiguus*	11	3	21.43%
		Gobiomys neimongolensis	3	2	14.28%
	Dipodidae	*Allosminthus gobiensis*	10	3	21.43%
		Allosminthus cf. *A. majusculus*	4	1	7.14%
		Allosminthus erons	4	2	14.28%
	Cricetidae	*Eocricetodon* sp.	7	3	21.43%
Middle White	Ctenodactyloidea	*Gobiomys neimongolensis*	11	4	33.33%
	Dipodidae	*Allosminthus gobiensis*	21	4	33.33%
		Sinosminthus sp.	1	1	8.33%
	Cricetidae	*Pappocricetodon schaubi*	2	1	8.33%
		Eucricetodon cf *E. wangae*	3	2	16.66%
Upper Red	Ctenodactyloidea	*Gobiomys exiguus*	13	4	8.89%
		Gobiomys neimongolensis	29	6	13.33%
	Dipodidae	*Allosminthus gobiensis*	8	3	6.67%

		Allosminthus cf. *A. majusculus*	29	6	13.33%
		Allosminthus ernos	42	9	20%
		Heosminthus nomogenesis	13	3	6.67%
		Sinosminthus sp.	3	2	4.44%
	Cricetidae	*Pappocricetodon siziwangqiensis*	1	1	2.22%
		Eucricetodon wangae	58	9	20%
		Eucricetodon sp.	7	2	4.44%
Upper White	Cricetidae	*Cricetops dormitor*	3	3	100%